Doping- and irradiation-controlled pinning of vortices in $BaFe_2(As_{1−x}P_x)_2$ single crystals

L. Fang,[1] Y. Jia,[1] J. A. Schlueter,[1] A. Kayani,[2] Z. L. Xiao,[1] H. Claus,[1] U. Welp,[1] A. E. Koshelev,[1]
G. W. Crabtree,[1] and W.-K. Kwok[1]

[1]*Materials Science Division, Argonne National Laboratory, Argonne, Illinois 60439, USA*
[2]*Physics Department, Western Michigan University, Kalamazoo, Michigan 49008, USA*
(Received 26 July 2011; revised manuscript received 12 September 2011; published 13 October 2011)

We report on the systematic evolution of vortex pinning behavior in isovalent doped single crystals of $BaFe_2(As_{1−x}P_x)_2$. Proceeding from optimal doped to overdoped samples, we find a clear transformation of the magnetization hysteresis from a fishtail behavior to a distinct peak effect, followed by a reversible magnetization and Bean-Livingston surface barriers. Strong point pinning dominates the vortex behavior at low fields whereas weak collective pinning determines the behavior at higher fields. In addition to doping effects, we show that particle irradiation by energetic protons can tune vortex pinning in these materials.

The discovery of multiband superconductivity in iron pnictides[1] with relatively high transition temperatures and modest superconducting anisotropy has opened unique research approaches for realizing an isotropic high T_C superconductor. These materials share, as a common structural motif, superconducting FeAs or FeSe/Te layers. Generally, superconductivity emerges from a semimetallic antiferromagnetic parent compound,[2] upon electron, hole, or isovalent doping, $BaFe_2(As_{1−x}P_x)_2$ being an example of the latter.[3] A key feature that can strongly affect the behavior of multiband superconductors is the interplay of inter- and intraband electron scattering. The scattering mechanism does not only affect the superconducting gap structure,[4] the temperature dependence of thermodynamic quantities such as the upper critical field,[5] and the superfluid density,[6] but also the pinning of superconducting vortices.[7] The charged dopant sites in electron- and hole-doped materials create strong scattering potentials that dominate electron scattering. In contrast, in isovalent doped $BaFe_2(As_{1−x}P_x)_2$ (BFAP), scattering can be tuned from the clean limit to the dirty limit; in pristine strongly overdoped BFAP, de Haas–van Alphen experiments have revealed long electron mean free paths.[8,9]

In this Rapid Communication, we report on a systematic study of vortex pinning in a series of doped BFAP crystals. We find a pronounced magnetization fishtail behavior, which evolves into a peak effect (PE) in the critical current with increased phosphorus doping. With further doping, vortex pinning becomes virtually negligible, leaving only the Bean-Livingston (BL) barrier as a source of vortex pinning, underlining the purity of the sample with a high phosphorus content. We demonstrate that strong point pinning (SPP) dominates at low magnetic fields, whereas weak collective pinning (WCP) occurs at high fields. In addition to doping effects, we show that irradiation by protons can tune the vortex pinning behavior in these materials.

High-purity $BaFe_2(As_{1−x}P_x)_2$ ($x = 0.32–0.6$) single crystals were grown using a self-flux method. The elemental composition was determined using x-ray energy dispersion spectra. The crystals were cut into a rectangular shape with a size $\sim 400 \times 300\ \mu m^2$ for magnetization and resistivity measurements. The upper critical field H_{C2} was determined from linear extrapolations of the temperature-dependent reversible magne-

tization to the normal-state baseline. The irreversibility field H_{irr} was determined from the first separation point between the zero-field-cooled and field-cooled magnetization curves. The critical current density (j_C) was estimated using the Bean critical-state model. In the case of dominant surface pinning, supercurrents are concentrated at the sample surface. We nevertheless calculated j_C values for comparison of the field dependence among samples. One overdoped crystal ($x = 0.55$) was irradiated at the tandem accelerator at Western Michigan University with 2-MeV protons to a dose of $8 \times 10^{15}\ p/cm^2$.

The inset of Fig. 1 shows the temperature-dependent magnetization curves for doping from $x = 0.32$ to 0.6. Except for $x = 0.6$, the transition widths of the crystals are very sharp with $\Delta T_C (10\%–90\%) < 1$ K. The corresponding resistivity curves are shown in the main panel. The residual resistivity decreases strongly upon P doping, from 30 to less than 5 $\mu\Omega$ cm, underlining the increased purity of the overdoped samples. Figure 2(a) displays the field-dependent magnetization for the optimal doping ($x = 0.32$) at various temperatures. The magnetization shows a sharp peak centered at zero field, as observed in most studies on the FeAs superconductors and, in contrast to a previous study,[10] a broad maximum, indicative of the "fishtail" effect at high fields. The fishtail peak moves to lower fields with increasing temperature. The field and temperature dependence of the fishtail is similar to that observed in other pnictides.[11–16] With increasing phosphorus doping ($x = 0.5$), the magnetization hysteresis curve collapses and becomes asymmetric, and nearly reversible at intermediate fields, followed by a pronounced PE at higher fields, as shown in Fig. 2(b). The PE moves to lower fields and its magnitude diminishes with increasing temperature. No PE was observed when the field was applied parallel to the crystal's *ab* plane. With further phosphorus doping, $x = 0.55$, the PE disappears and the magnetization hysteresis curve at $T = 5$ K becomes almost reversible over its entire field range up to the upper critical field. Furthermore, the descending field branch of the magnetization curve shows nearly zero magnetization. Such behavior has been observed in very clean $YBa_2Cu_3O_{6+\delta}$ crystals and was considered as a fingerprint of vortex pinning by the BL surface barrier,[17,18] which becomes the dominant pinning mechanism at high fields when vortices are straight in the absence of bulk pinning.
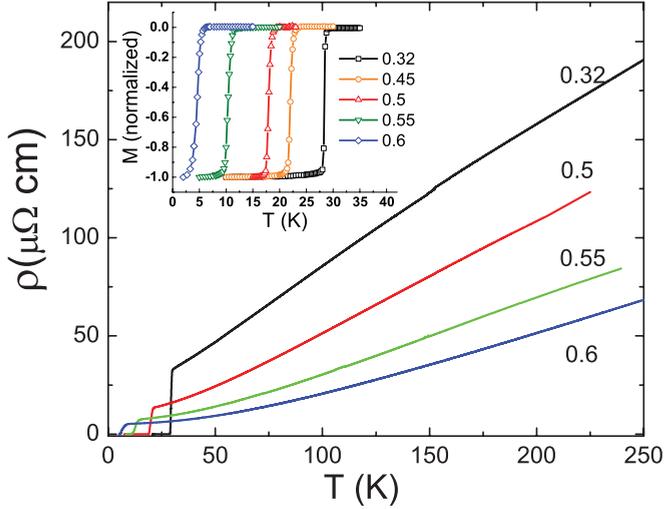
FIG. 1. (Color online) Temperature dependence of the resistivity in zero field for BFAP. (inset) Superconducting diamagnetic transition of $BaFe_2(As_{1-x}P_x)_2$ crystals ($0.32 \leqslant x \leqslant 0.6$) measured at $H \parallel c = 10$ Oe.

Figure 2(d) compares the critical currents $j_C(H)$ of all the phosphorus-doped crystals obtained at the *same reduced temperature* $T/T_C \approx 0.55$. A common feature displayed in Fig. 2(d) is the $H^{-0.5}$ dependence at low fields below $H < 0.3$ T and the $H^{-0.7}$ to H^{-1} dependencies at higher fields for the $0.32 < x < 0.5$ samples. These $j_C(H)$ behaviors are consistent with SPP theory.[19] In the simplest case when all pins are occupied by vortices, $j_C = \frac{n_p f_{pin}}{B}$, where n_p is the volume concentration of effective pinning centers, f_{pin} is the maximum value of pinning force on one defect, and B is the magnetic induction. At smaller fields when interaction between vortices prevents occupation of all pin sites, $F = \Phi_0 j_C = \varepsilon_0 n_p b \sqrt{\frac{\Phi_0}{B}}$, where Φ_0 is the flux quantum, b is the size of the pinning defect and is assumed to be greater than coherence ξ, $\varepsilon_0 = \Phi_0^2/4\pi \mu_0 \lambda_{ab}^2$ is the characteristic vortex energy per unit length, μ_0 is the magnetic constant, and λ is the penetration depth. Hence both H^{-1} and $H^{-0.5}$ relations can be accounted for by SPP. Similar SPP behavior has been observed recently in several 122- and 1111-based pnictides at fields below the appearance of the fishtail behavior.[10,11] In elevated fields, typically larger than 1 T, SPP becomes

negligible and is overtaken by collective pinning, as evidenced by the observation of a fishtail at optimal doping and a PE with at higher phosphorus concentration [see Fig. 2(d)]. The fishtail and PE are typically associated with a large concentration of weak pinning sites, leading to collective pinning behavior.

A $1/H$ dependence of J_C is also observed for the highly overdoped samples, albeit at very low J_C values. This behavior is expected for BL barrier pinning,[20] where $m \approx H_p^2/2B$, with m the magnetic moment on the ascending branch, and H_p is the first field of flux penetration. Thus, considering the shape of the magnetic hysteresis of the $x = 0.55$ sample, the $1/H$ dependence is associated with the BL barrier instead of SPP. Figure 2(d) also shows that J_C drops strongly from $\sim 4 \times 10^5$ A/cm^2 to $\sim 2 \times 10^4$ A/cm^2 (at reduced temperatures of $T/T_C = 0.55$) in going from $x = 0.32$ to $x = 0.5$ when bulk pinning is dominant. The J_C value for $x = 0.32$ is in good agreement with a previous report.[21] The doping dependence of J_C is also consistent with recent de Haas–van Alphen measurements in overdoped BFAP that reported an increase in the mean free path with phosphorus doping.[8,9] However, it differs from a report in which a higher J_C was found for a $x = 0.49$ sample than for $x = 0.32$ at $T/T_C = 0.3$.[10]

To test whether irradiation-induced defects could mimic the effect of vortex behavior due to phosphorus doping, we irradiated the pristine $x = 0.55$ crystal, which showed essentially no bulk pinning [see Fig. 2(c)]. Figure 2(c) shows the magnetic hysteresis curve obtained at 5 K on the same sample after irradiation. The magnetization hysteresis is enhanced considerably compared to that of the pristine crystal, indicating that the p-irradiation-induced defects are effective pinning sites. The $M(H)$ curve does not display a discernible fishtail, and the extent of the enhanced pinning at low fields is strongly reduced as compared with the data in Fig. 2(a), for instance.

Figure 3 shows the phase diagram as deduced from temperature-dependent magnetization measurements. We determine the slope of the upper critical field of $\mu_0 dH_{C2}/dT = -0.86$ T/K, in good agreement with results of our specific-heat measurements. The phase diagram is characterized by a narrow vortex liquid region between H_{C2} and H_{irr}, and by the occurrence of the peak effect just below H_{irr}. These characteristics strongly resemble those of MgB$_2$.[22,23] However, on our current samples neither the resistivity nor the magnetization displays a
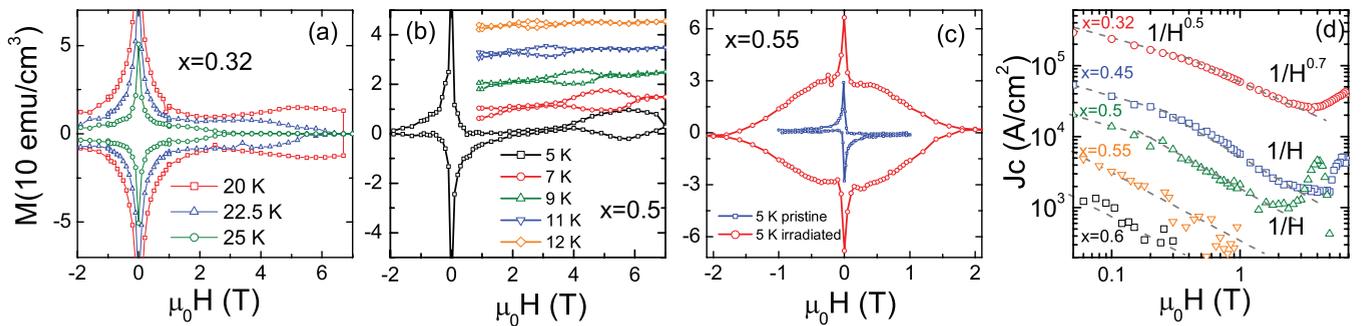

FIG. 2. (Color online) Magnetization hysteresis of (a) optimum doped ($x = 0.32$) BFAP, (b) overdoped ($x = 0.5$) (note the curves for different temperatures are shifted for clarity), and (c) pristine and proton-irradiated overdoped ($x = 0.55$) crystals for $H \parallel c$. (d) $j_C(H)$ for optimal and overdoped crystals measured at the same reduced temperature $T/T_C \cong 0.55$. The dashed lines are guides to the eye.
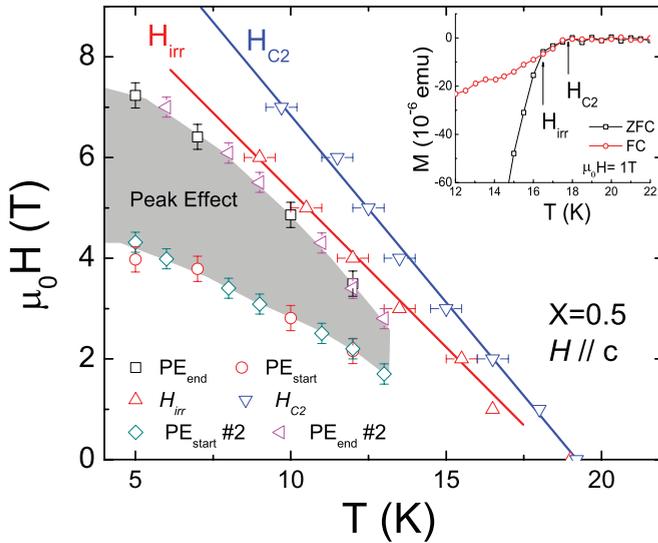
FIG. 3. (Color online) Phase diagram of the $x = 0.5$ sample. The inset shows the determination of the upper critical field and the irreversibility field through field cooling and zero-field-cooled temperature-dependent magnetization curves.
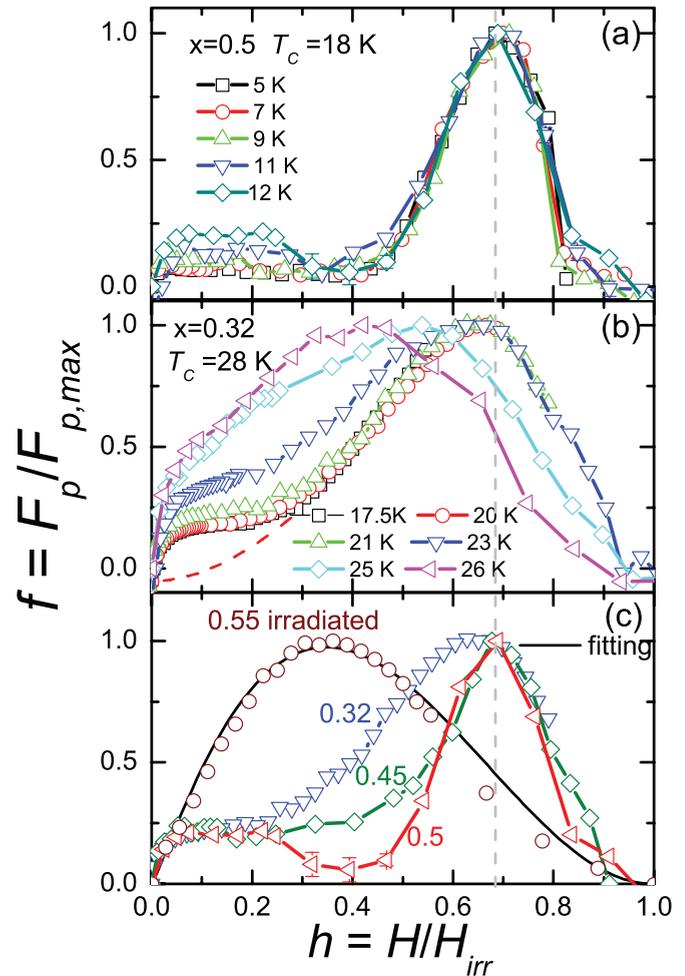

FIG. 4. (Color online) (a) Normalized pinning force as a function of reduced field for BFAP with $x = 0.5$ at various temperatures, and (b) with $x = 0.32$. The dotted red line is a guide to the eye, indicating the contribution due to collective pinning to the pinning force. (c) Comparison of $f(h)$ among various phosphorus-doped samples and a proton-irradiated $x = 0.55$ sample at $T/T_C = 0.66$.

discontinuous temperature dependence that could be indicative of a first-order vortex transition.

Plots of the normalized pinning force ($f = F_p/F_{p,\max}$, $F_p = \mu_0 H j_C$) as a function of reduced field ($h = H/H_{irr}$) have proven useful for identifying various pinning regimes.[13,16,24] The pinning force curves for $x = 0.5$ [Fig. 4(a)] are characterized by a sharp maximum near $h = 0.7$ (corresponding to the PE) and a plateau at $h < 0.2$ corresponding to the approximate $1/H$ dependence of j_C, and thus representing the regime of SPP. The curves in the PE region display remarkable scaling for different temperatures. At temperatures above 12 K the PE disappears and the magnetization in high fields becomes reversible. For the $x = 0.32$ sample we observe a similar, albeit broader, maximum at approximately $h = 0.7$, corresponding to the fishtail in the magnetization. The plateau at $h < 0.2$ as well as the steep rise at very low fields represent the strong point pinning regime, since the initial $j_C \sim H^{-1/2}$ dependence would correspond to a square-root rise in the pinning force. The pinning force curves scale well at temperatures below 23 K, however, this scaling breaks down at the highest temperatures and the $f(h)$ curves acquire a more symmetric shape. Figure 4(c) displays the progression of the $f(h)$ for various doping levels at $T/T_C = 0.66$. These results indicate that starting from a certain degree of bulk pinning, here achieved in the sample with $x = 0.5$ at temperatures below 13 K, a sharp peak effect appears near the irreversibility line. With increased bulk pinning this peak effect widens into the fishtail feature in the magnetization hysteresis. It is a remarkable feature of BFAP that, over large sections of the H-T-x diagram, pinning can be separated into two distinct mechanisms: strong point pinning at low fields and collective pinning at high fields. Even though critical currents due to different pinning mechanisms are not simply additive in general, the data in Fig. 4(b) suggest that the pinning force due to the collective pinning mechanism is negligible at low fields.

Also included in Fig. 4(c) is the pinning force curve of the p-irradiated $x = 0.55$ sample. It has a conventional shape with no signs of strong point pinning at low fields, and is fitted well by the relation $h(1-h)^2$. This type of pinning force curve is expected for pinning by normal point pins (δT_C pinning). In general, however, the pinning force curves in Fig. 4 do not follow the standard forms.[24] It is nevertheless instructive to note that a maximum of the pinning force near $h \sim 0.7$ is indicative for $\delta\kappa$ (δl) pinning. This pinning mechanism has been invoked in a previous analysis[11,21] of the pinning properties of 1111- and 122-based samples. It is likely to arise due to fluctuations in the electron mean free path caused by inhomogeneity in the dopant distribution. As the sample temperature approaches T_C, variations in T_C become relatively more important, leading to areas of suppressed condensation energy or normal regions. In this case δT_C pinning is expected, characterized by a maximum in the pinning force curve near 0.35. This scenario can account for the temperature evolution of the pinning force curves of the $x = 0.32$ sample, and the results for the p-irradiated sample, if one assumes

that the irradiation-induced defects are regions of suppressed superconductivity.[25] Upon increasing temperature, the $x = 0.5$ (and 0.45) sample transitions into the state of the $x = 0.55$ sample, that is, vanishing bulk pinning before the regime of δT_C pinning can be reached.

These general features are not limited to BFAP but arise in materials that can be synthesized with fairly high purity, such as MgB_2. Neutron as well as electron irradiation studies on MgB_2 crystals have also shown the transformation from a virtually reversible magnetization curve in clean MgB_2 crystals into a PE and eventually into a fishtail-shaped magnetization.[23,26] Our data clearly demonstrates that the PE emerges from the fishtail magnetization, once pinning is reduced via phosphorus doping. Conversely, the large

magnetization hysteresis can be recovered by introducing point (or cluster) defects via proton irradiation. Our studies also point to the possibility of separating the effects of strong and weak collective pinning via doping and controlled proton irradiation.

[1] Y. Kamihara, H. Hiramatsu, M. Hirano, R. Kawamura, H. Yanagi, T. Kamiya, and H. Hosono, J. Am. Chem. Soc. **128**, 10012 (2006).

[2] D. C. Johnston, Adv. Phys. **59**, 803 (2010); J. Paglione and R. L. Greene, Nat. Phys. **6**, 645 (2010); P. C. Canfield and S. L. Bud'ko, Annu. Rev. Condens. Matter Phys. **1**, 27 (2010); P. J. Hirschfeld, M. M. Korshunov, and I. I. Mazin, e-print arXiv:1106.3712.

[3] S. Jiang, H. Xing, G. F. Xuan, C. Wang, Z. Ren, C. M. Feng, J. H. Dai, Z. A. Xu, and G. H. Cao, J. Phys. Condens. Matter **21**, 382203 (2009); S. Kasahara, T. Shibauchi, K. Hashimoto, K. Ikada, S. Tonegawa, R. Okazaki, H. Shishido, H. Ikeda, H. Takeya, K. Hirata, T. Terashima, and Y. Matsuda, Phys. Rev. B **81**, 184519 (2010).

[4] A. Glatz and A. E. Koshelev, Phys. Rev. B **82**, 012507 (2010); H. Kontani and S. Onari, Phys. Rev. Lett. **104**, 157001 (2010); S. Onari and H. Kontani, *ibid.* **103**, 177001 (2009).

[5] J. Jaroszynski, F. Hunte, L. Balicas, Youn-jung Jo, I. Raičević, A. Gurevich, D. C. Larbalestier, F. F. Balakirev, L. Fang, P. Cheng, Y. Jia, and H. H. Wen, Phys. Rev. B **78**, 174523 (2008); A. A. Golubov and A. E. Koshelev, *ibid.* **68**, 104503 (2003); A. Gurevich, *ibid.* **67**, 184515 (2003).

[6] V. G. Kogan, Phys. Rev. B **80**, 214532 (2009); A. B. Vorontsov, M. G. Vavilov, and A. V. Chubukov, *ibid.* **79**, 140507 (2009); R. Prozorov and V. G. Kogan, e-print arXiv:1107.0675.

[7] E. V. Thuneberg, J. Kurkijarvi, and D. Rainer, Phys. Rev. Lett. **48**, 1853 (1982); Phys. Rev. B **29**, 3913 (1984); C. J. van der Beek and P. H. Kes, *ibid.* **43**, 13032 (1991).

[8] H. Shishido, A. F. Bangura, A. I. Coldea, S. Tonegawa, K. Hashimoto, S. Kasahara, P. M. C. Rourke, H. Ikeda, T. Terashima, R. Settai, Y. Onuki, D. Vignolles, C. Proust, B. Vignolle, A. McCollam, Y. Matsuda, T. Shibauchi, and A. Carrington, Phys. Rev. Lett. **104**, 057008 (2010); B. J. Arnold, S. Kasahara, A. I. Coldea, T. Terashima, Y. Matsuda, T. Shibauchi, and A. Carrington, Phys. Rev. B **83**, 220504 (2011).

[9] J. G. Analytis, J. H. Chu, R. D. McDonald, S. C. Riggs, and I. R. Fisher, Phys. Rev. Lett. **105**, 207004 (2010).

[10] C. J. vanderBeek, M. Konczykowski, S. Kasahara, T. Terashima, R. Okazaki, T. Shibauchi, and Y. Matsuda Phys. Rev. Lett. **105**, 267002 (2010).

[11] C. J. van der Beek, G. Rizza, M. Konczykowski, P. Fertey, I. Monnet, Thierry Klein, R. Okazaki, M. Ishikado, H. Kito, A. Iyo, H. Eisaki, S. Shamoto, M. E. Tillman, S. L. Bud'ko, P. C.

Canfield, T. Shibauchi, and Y. Matsuda, Phys. Rev. B **81**, 174517 (2010).

[12] R. Prozorov, N. Ni, M. A. Tanatar, V. G. Kogan, R. T. Gordon, C. Martin, E. C. Blomberg, P. Prommapan, J. Q. Yan, S. L. Bud'ko, and P. C. Canfield, Phys. Rev. B **78**, 224506 (2008).

[13] H. Yang, H. Q. Luo, Z. S. Wang, and H. H. Wen, Appl. Phys. Lett. **93**, 142506 (2008).

[14] B. Shen, P. Cheng, Z. Wang, L. Fang, C. Ren, L. Shan, and H. H. Wen, Phys. Rev. B **81**, 014503 (2010).

[15] S. Salem-Sugui, L. Ghivelder, A. D. Alvarenga, L. F. Cohen, K. A. Yates, K. Morrison, J. L. Pimentel, H. Luo, Z. Wang, and H. H. Wen, Phys. Rev. B **82**, 054513 (2010).

[16] A. Yamamoto *et al.*, Appl. Phys. Lett. **94**, 062511 (2009).

[17] M. Konczykowski, L. I. Burlachkov, Y. Yeshurun, and F. Holtzberg, Phys. Rev. B **43**, 13707 (1991).

[18] J. R. Clem, in *Proceedings of the LT 13*, edited by K. D. Timmerhaus, W. J. O'Sullivan, and E. F. Hammel (Plenum, New York, 1974), Vol. 3, p. 102.

[19] Yu. N. Ovchinnikov and B. I. Ivlev, Phys. Rev. B **43**, 8024 (1991); G. Blatter, V. B. Geshkenbein, and J. A. G. Koopmann, Phys. Rev. Lett. **92**, 067009 (2004); A. E. Koshelev and A. B. Kolton, e-print arXiv:1106.2477.

[20] L. Burlachkov, Phys. Rev. B **47**, 8056 (1993).

[21] S. V. Chong, S. Hashimoto, and K. Kadowaki, Solid State Commun. **150**, 1178 (2010).

[22] M. Pissas, S. Lee, A. Yamamoto, and S. Tajima, Phys. Rev. Lett. **89**, 097002 (2002).

[23] T. Klein, R. Marlaud, C. Marcenat, H. Cercellier, M. Konczykowski, C. J. vanderBeek, V. Mosser, H. S. Lee, and S. I. Lee, Phys. Rev. Lett. **105**, 047001 (2010).

[24] D. Dew-Hughes, Philos. Mag. **30**, 293 (1974); E. J. Kramer, J. Appl. Phys. **44**, 1360 (1973); H. Yamasaki, K. Endo, S. Kosaka, M. Umeda, S. Yoshida, and K. Kajimura, Phys. Rev. Lett. **70**, 3331 (1993); M. R. Koblischka, A. J. J. van Dalen, T. Higuchi, S. I. Yoo, and M. Murakami, Phys. Rev. B **58**, 2863 (1998).

[25] Proton irradiation in YBCO was shown to produce point defects (∼70%) and small cluster defects (∼30%) [A. M. Petrean, L. M. Paulius, W. K. Kwok, J. A. Fendrich, and G. W. Crabtree, Phys. Rev. Lett. **84**, 5852 (2000)].

[26] M. Zehetmayer, M. Eisterer, J. Jun, S. M. Kazakov, J. Karpinski, B. Birajdar, O. Eibl, and H. W. Weber, Phys. Rev. B **69**, 054510 (2004).